

A Dynamical Model for the Evolution of Hot Spots in Powerful Radio Sources

M. Perucho and J. M. Martí

Departamento de Astronomía y Astrofísica, Universidad de Valencia,
Dr. Moliner 50, 46100 Burjassot (Valencia), Spain
manuel.perucho@uv.es
jose-maria.marti@uv.es

Received 2002 June 22, accepted 2003 January 13

Abstract: Compact symmetric objects are considered the young counterparts of large doubles according to advance speeds measured or inferred from spectral ageing. Here we present a simple power law model for the CSO/FR II evolution based on the study of sources with well defined hot spots. The luminosity of the hot spots is estimated under minimum energy conditions. The advance of the source is considered to proceed in ram pressure equilibrium with the ambient medium. Finally, we also assume that the jets feeding the hot spots are relativistic and have a time dependent power. Comparison with observational data points to an interpretation of the CSO–FR II evolution in terms of decreasing jet power with time.

Keywords: galaxies: active — galaxies: jets — galaxies: ISM — radio continuum: galaxies

1 Introduction

Compact symmetric objects (CSOs) are thought to be the early stages of powerful, extended radio sources; this was first suggested by Phillips & Mutel (1982) and later established by Readhead et al. (1996). This view has been underpinned by recent measurements of hot spot advance speeds (Owsianik & Conway 1998; Owsianik et al. 1998; Taylor et al. 2000; Tschager et al. 2000; Polatidis & Conway 2003) and spectral ageing studies (Murgia 2003).

Current evolutionary models (see Fanti & Fanti 2002) relate luminosity and expansion velocity of a source to jet power and external gas density. The energy accumulated in the lobes drives the source expansion. Ram pressure equilibrium with the ambient medium is assumed. The volume of the source is usually inferred from self-similarity arguments whereas radio power is computed from equipartition assumptions. In all the models, jet power was considered to be constant.

Here we discuss a model of the time dependent jet power model for CSOs introduced in Perucho & Martí (2002a, Paper I) and Perucho & Martí (2002b, Paper II), which describes the long term evolution of powerful radio sources. In order to avoid conjecture about the volume growth of the source (e.g. self-similarity), we concentrate on hot spots for which properties like size or luminosity can reliably be derived. In our model we assume that the advance work of the hot spot is directly connected to the jet power. The remaining assumptions of our model are standard: The luminosity of the hot spot is estimated under minimum energy conditions, the advance of the hot spot proceeds in ram pressure equilibrium with the ambient medium, and the jets feeding the hot spots are relativistic.

In section 2 we give the main equations derived from the model. In section 3 we present the observational data used

to derive our model, and section 4 is devoted to discussion and conclusions drawn from this work.

2 A dynamical model for the evolution of hot spots in powerful radio sources

Our model relies on three basic parameters, β , δ , and ε . The first (β) is the exponent for the growth of linear size, r of a hot spot with time, $r_{\text{hs}} \propto t^\beta$, as it propagates through an external medium, the density of which varies with linear size (LS) as $\rho_{\text{ext}} \propto (LS)^{-\delta}$.

Using the hot spot advance speed, we can relate linear size (LS) with time and describe the evolution of physical parameters in terms of distance to the source of the jets feeding them. Considering that hot spots advance with non-relativistic speeds, v_{hs} , ram pressure equilibrium leads to,

$$v_{\text{hs}} = \sqrt{\frac{F_j}{A_{j,\text{hs}}\rho_{\text{ext}}}}, \quad (1)$$

where F_j is the jet thrust and $A_{j,\text{hs}}$ the cross-sectional area of the jet at the hot spot, assumed to be proportional to r_{hs}^2 .

The final step is to consider that for a relativistic jet, the thrust and power, Q_j , are simply related by $F_j \approx Q_j/c$. If we now allow for a dependence of the jet power with time ($Q_j \propto t^\varepsilon$), combine all the dependencies and integrate, we get

$$v_{\text{hs}} \propto (LS)^{\delta/2} t^{\varepsilon/2 - \beta} \rightarrow t \propto (LS)^{(1-\delta/2)/(\varepsilon/2+1-\beta)}. \quad (2)$$

Substituting in the expressions for the hot spot radius and speed, we obtain

$$\begin{aligned} r_{\text{hs}} &\propto (LS)^{\beta(1-\delta/2)/(\varepsilon/2+1-\beta)}, \\ v_{\text{hs}} &\propto (LS)^{(\delta/2+\varepsilon/2-\beta)/(\varepsilon/2+1-\beta)}. \end{aligned} \quad (3)$$

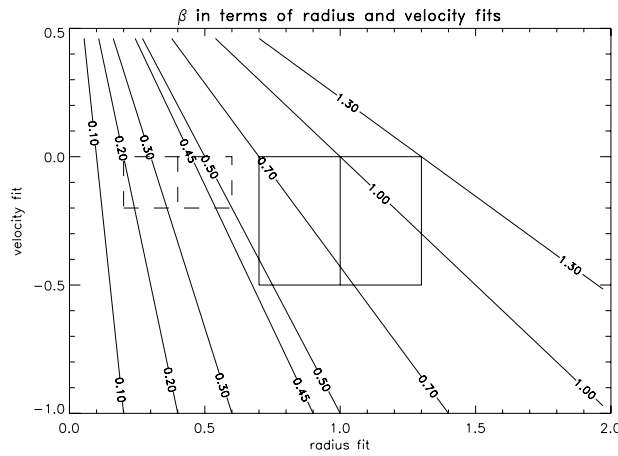


Figure 1 Contours of β as a function of s_v and s_r for the model discussed in the text. Boxes bound the expected values of β for CSO-MSO evolution (—) and MSO-FR II evolution (----).

The next equation in our model comes from the source energy balance. We assume that the power consumed by the source in the hot spot advance, $(P\dot{V})_{hs,adv}$, adjusts to the evolution of the jet kinetic power, i.e.,

$$(P\dot{V})_{hs,adv} (\propto P_{hs} r_{hs}^2 v_{hs}) \propto Q_j \propto t^\epsilon. \quad (4)$$

Finally, under the assumption of minimum energy, the luminosity of the hot spot ($L_{hs} \propto P_{hs}^{7/4} r_{hs}^3$) may be expressed in terms of LS

$$L_{hs} \propto (LS)^{(7/4[-\delta/2(\epsilon-2\beta)+\epsilon/2-\delta/2-\beta]+3\beta(1-\delta/2)]/(\epsilon/2-\beta+1)}. \quad (5)$$

Inverting equations (3) and (5), we derive expressions for the evolution parameters of our model in terms of exponents for the evolution of observable quantities.

$$\beta = \frac{s_r}{1-s_v}, \quad \delta = \frac{12}{7}s_r - \frac{4}{7}s_L + s_v, \quad (6)$$

$$\epsilon = \frac{\frac{2}{7}s_r + \frac{4}{7}s_L + s_v}{1-s_v},$$

where s_r , s_v and s_L stand for the values of the exponents of the observed hot spot radius, advance velocity and luminosity as functions of LS . Figure 1 shows the variation of β , and Figure 2 that of δ and ϵ with the different exponents. Note that the previous expressions not only provide a system of algebraic equations to obtain values for the theoretical parameters in our model, they also prove that our model is self-consistent since the variations of the theoretical parameters inferred from observations agree with physical expectations. Therefore, if we are able to obtain values for the exponents in equations (3) and (5) from observational data, assuming that the corresponding $LS-L_{hs}$ and $LS-r_{hs}$ plots track the evolution of individual sources, we can derive expected values for β , δ and ϵ from the observational fits.

3 Observables from hot spots

In order to apply our model to the evolution of powerful radio sources from the CSO to the FR II phase, we have

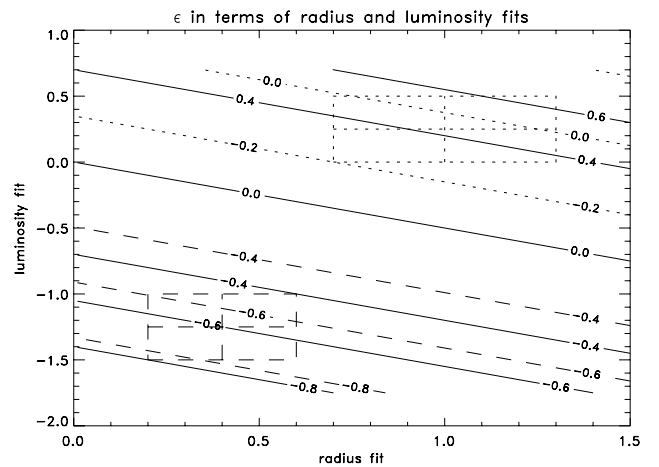
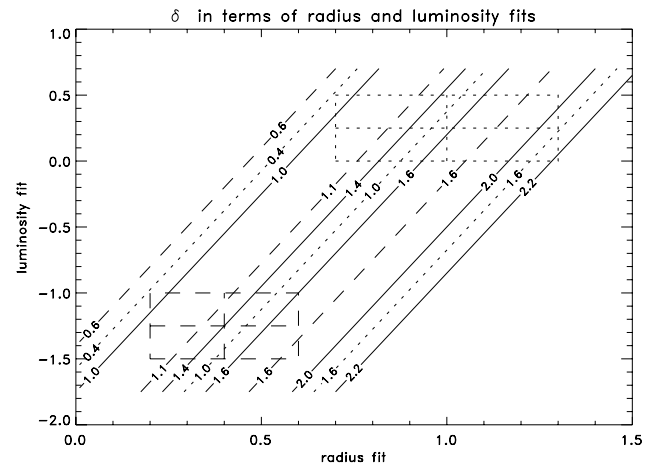


Figure 2 Contours of δ and ϵ as function of s_r and s_L for the model discussed in the text and different slopes for the hot spot expansion (continuous contours: $s_v = 0$; dotted contours: $s_v = -0.5$; dashed: $s_v = -0.2$). Boxes bound the expected values of δ and ϵ for CSO-MSO evolution (.....) and MSO-FR II evolution (----).

compiled a sample of sources with well defined hot spots and linear sizes between tens of parsecs to hundreds of kiloparsecs. The sample of CSO is the same as the one used in Paper I. Sources were selected from the GPS samples of Stanghellini et al. (1997), Snellen et al. (1998, 2000) and Peck & Taylor (2000). We have chosen sources with double morphology already classified in the literature as CSOs and also those whose components can be safely interpreted as hot spots even though the central core has not been identified yet. The criteria we have followed are quite similar to those used by Peck & Taylor (2000) (see Paper I for details). Seven *medium size* (1–10 kpc) symmetric objects (‘doubles’) have been taken from the CSS-3CR sample of Fanti et al. (1985). Finally, 40 sources from the sample of FR II-3CR radio galaxies of Hardcastle et al. (1998) have been considered (see Paper I for further details).

All the subsamples in our combined sample have similar flux density cut-offs: 1 Jy at 5 GHz for the CSOs and 10 Jy at 178 MHz for the MSOs and FR IIs. The differences in redshift among the three subsamples ($z \leq 1$ for the CSOs; $0.3 < z < 1.6$ for the MSOs; $z < 0.3$ for the

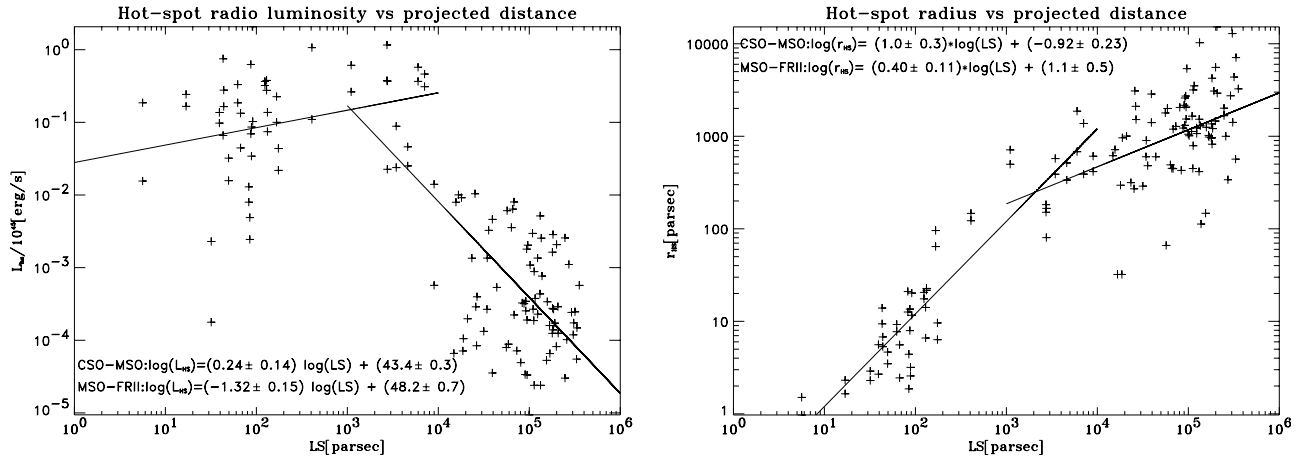


Figure 3 Log–log plot for the hot spot radius and luminosity versus projected linear size for the sources in the combined sample. Continuous lines correspond to the best linear fits for both CSO–MSO and MSO–FR II subsamples.

Table 1. Best fits for radius (s_r) and luminosity (s_L), along with their errors and correlation coefficients (r). In the right part of the table we write the values of the evolution parameters (β , δ and ε) which result from the calculated best fits and two different possible slopes for advance speed (s_v), along with their errors, which are directly taken from Figures 1 and 2 for β , δ and ε

	r_{hs}		L_{hs}		Model	β	δ	ε
	s_r	r	s_L	r				
CSO–MSO	1.0 ± 0.3	0.93	0.24 ± 0.14	0.26	0	1.0 ± 0.3	1.6 ± 0.6	0.4 ± 0.2
					–0.5	0.7 ± 0.2	1.1 ± 0.7	-0.05 ± 0.15
MSO–FR II	0.40 ± 0.11	0.51	-1.32 ± 0.15	–0.69	0	0.4 ± 0.2	1.4 ± 0.5	-0.6 ± 0.2
					–0.2	0.3 ± 0.2	1.2 ± 0.5	-0.75 ± 0.15

FR IIs) enhances the luminosity drop between MSOs and FR IIs.

Figure 3 displays the hot spot radius and luminosity with respect to projected linear size on logarithmic scales, together with the best linear fit for both CSO–MSO and MSO–FR II subsamples. Hot spot linear sizes and luminosities have been calculated as explained in the Appendix of Paper I. Table 1 lists the slopes characterizing the power law fits and their errors, as well as the correlation coefficients.

4 Discussion

Assuming an evolutionary interpretation, the plots in Figure 3 show a most remarkable self-similar growth of hot spot radius with linear size for the first 10 kpc of evolution and a flattening for large sources, in agreement with Jeyakumar & Saikia (2000). A change of sign of the slope for radio-luminosity is also seen at 10 kpc. This fact is consistent with the transition between the ISM and the IGM, also suggested by the disappearance of infrared aligned emission after the CSS stage (de Vries 2003), which could imply significant changes in the evolution.

Fits can be used to constrain the parameters β , δ and ε of the model. These values are listed in Table 1. As hot spots undergo a secular deceleration (from 0.2 c in the first kpc to a value approximately ten times smaller in FR IIs) and

there are no observational indications of any acceleration, hence constant and decreasing hot spot velocities have been considered for the CSO–MSO and MSO–FR II fits.

The break in the fits shown in Figure 3 at 1–10 kpc produces very different values for the parameters in the CSO–MSO and MSO–FR II phases. In contrast, there is a complete consistency between the fits for the CSOs alone (see Paper I) and those for the CSO–MSO phase. The hot spot expansion rate, β , decreases from ≈ 1 in the CSO–MSO phase to ≈ 0.4 in the MSO–FR II phase. Jet power increases with time during the first phase ($\varepsilon \approx 0, 0.4$) depending on the value chosen for s_v , and decreases in the long term ($\varepsilon \approx -0.6, -0.7$). It would be interesting to relate the time evolution of the jet power with the physical processes responsible for the jet production (i.e. accretion rate, black hole spin). The density profile is flat ($\delta < 2$), consistent for the CSO–MSO stage with that derived by Pihlstrom et al. (2003) ($\delta \simeq 1.3$) for GPS–CSS sources from H I detections. The transition between the two phases is smooth, although this can be a result of the fitting process that washes out any steep gradient between a flat ($\delta \approx 0$), small core and the intergalactic medium. We also note that the density gradient depends strongly on s_v , and that this parameter is poorly known. A value of $\delta = 2$ in the CSO–MSO phase will produce accelerating hot spots ($s_v = 0.5$) and a large increase of the jet power ($\varepsilon = 2$). Finally, fixing s_L and s_r and taking $\delta = 0$, we

get $s_v = -1.5$, which is too small to be maintained over a long distance: starting with a hot spot speed of $0.2c$ at 50 pc , the hot spot speed at 0.5 kpc would have decreased to $6 \times 10^{-3}c$, much smaller than the present accepted values for CSO advance speeds (Polatidis & Conway 2003; Murgia 2003). It would be interesting to have upper limits of hot spot advance speeds in CSOs in order to constrain the density profile and the jet power evolution.

Regarding the problem of trapped sources, a suitable configuration of external medium density and jet power evolution may lead to a number of sources which, along with core-jets, may contribute to the excess of small sources in number statistics (Marecki et al. 2003; Drake et al. 2003).

Acknowledgments

We thank Prof. R. Fanti for his interest in our work. This research was supported by Spanish Ministerio de Ciencia y Tecnología (grant AYA2001-3490-C02-01). M. P. thanks the University of Valencia for his fellowship within the V SEGLES program and also thanks LOC and SOC of the 3rd GPS–CSS Workshop for their kindness and hospitality.

References

- Drake, C. L., McGregor, P. J., Bicknell, G. V., & Dopita, M. A. 2003, *PASA*, 20, 57
- Fanti, C., Fanti, R., Parma, P., Schilizzi, R. T., & van Breugel, W. J. M. 1985, *A&A*, 143, 292
- Fanti, C., & Fanti, R. 2002, in *Issues in Unification of AGNs*, eds Maiolino, R., Marconi, A., Nagar, N. (ASP Conference Series)
- Hardcastle, M. J., Alexander, P., Pooley, G. G., & Riley, J. M. 1998, *MNRAS*, 296, 445
- Jeyakumar, S., & Saikia, D. J. 2000, *MNRAS*, 311, 397
- Marecki, A., Spencer, R. E., & Kunert M. 2003, *PASA*, 20, 46
- Murgia, M., 2003, *PASA*, 20, 19
- Owsianik, I., & Conway, J. E. 1998, *A&A*, 337, 69
- Owsianik, I., Conway, J. E., & Polatidis, A. G. 1998, *A&A*, 336L, 37
- Peck, A. B., & Taylor, G. B. 2000, *ApJ*, 534, 90
- Perucho, M., & Martí, J. M. 2002a, *ApJ*, 568, 639 (Paper I)
- Perucho, M., & Martí, J. M. 2002b, in preparation (Paper II)
- Phillips, R. B., & Mutel, R. L. 1982, *A&A*, 106, 21
- Pihlstrom, Y., Conway, J., Vermelen, R., 2003, *PASA*, 20, 62
- Polatidis, A. G., & Conway, J. E., 2003, *PASA*, 20, 69
- Readhead, A. C. S., Taylor, G. B., Xu, W., Pearson, T. J., Wilkinson, P. N., & Polatidis, A. G. 1996, *ApJ*, 460, 612
- Snellen, I. A. G., Schilizzi, R. T., de Bruyn, A. G., Miley, G. K., Rengelink, R. B., Rötgering, H. J. A., & Bremer, M. N. 1998, *A&AS*, 131, 435
- Snellen, I. A. G., Schilizzi, R. T., & van Langevelde, H. J. 2000, *MNRAS*, 319, 429
- Stanghellini, C., O’Dea, C. P., Baum, S. A., Dallacasa, D., Fanti, R., & Fanti, C. 1997, *A&A*, 325, 943
- Taylor, G. B., Marr, J. M., Pearson, T. J., & Readhead, A. C. S. 2000, *ApJ*, 541, 112
- Tschager, W., Schilizzi, R. T., Rötgering, H. J. A., Snellen, I. A. G., & Miley, G. K. 2000, *A&A*, 360, 887
- de Vries, W., 2003, *PASA*, 20, 6